

# A New Carrier-Phase Multipath Observable for GPS Real-Time Kinematics, Based on Between Receiver Dynamics

Luis Serrano, Donghyun Kim and Richard B. Langley  
*Department of Geodesy and Geomatics Engineering  
University of New Brunswick, Canada*

## BIOGRAPHIES

Luis Serrano obtained his Diploma in geographic engineering from the Faculty of Sciences of the University of Lisbon, Portugal. For 4 years he worked as a geodetic engineer in private companies. Currently he is a Ph.D. student in the Department of Geodesy and Geomatics Engineering at the University of New Brunswick, where he carries out research in real-time precise navigation in indoor/outdoor environments.

Donghyun Kim is a research associate in the Department of Geodesy and Geomatics Engineering at the University of New Brunswick, where he has developed the UNB RTK software for a gantry crane auto-steering system. He has a B.Sc., M.Sc., and Ph.D. in geomatics from Seoul National University. He has been involved in GPS research since 1991. Currently, Dr. Kim carries out research related to ultrahigh-performance RTK positioning at up to a 50 Hz data rate, with application to real-time deformation monitoring, Internet-based moving platform tracking, and machine control.

Richard B. Langley is a professor in the Department of Geodesy and Geomatics Engineering at the University of New Brunswick, where he has been teaching and conducting research since 1981. He has a B.Sc. in applied physics from the University of Waterloo and a Ph.D. in experimental space science from York University, Toronto. Professor Langley has been active in the development of GPS error models since the early 1980s and is a contributing editor and columnist for GPS World magazine.

## ABSTRACT

In GPS differential carrier-phase measurements, multipath is still present and remains as the major contribution to the error budget, especially the low-frequency, short-delay multipath (specular). There are various approaches to mitigate this effect. The most notable is to build a multipath profile (also called an effective reflector) and to

parameterize the multipath measurements that resemble the geometry between the GPS receiver and the profile.

However, problems still remain in this approach since the basic measurements used for the estimators do not entirely correspond to all the physical effects of multipath. SNR measurements are used extensively due to their high correlation with the multipath environment and the receiver-satellite geometry. Due to their low precision, however, estimators converge over a long time span. Thus, they turn out to be an impractical measurement for real-time applications. On the other hand, methods to derive and separate the multipath that filter or use the carrier phase, not only may mask out the platform dynamics (especially when higher dynamics are involved), but also may introduce other unexpected biases.

These limitations lead us to derive multipath observables for multipath mitigation, merging the synergies from previous approaches. The multipath observables will carry all the multipath spectra with no limitation on the number of multipath signals (including specular reflections and diffraction), and be used as a technique that does not require *a priori* knowledge of the environment. Since the multipath observables will be derived from the platform dynamics (i.e., GPS carrier-phase derived velocity and acceleration estimates that can be designed to be immune to multipath), they can give a good signature of the low-frequency multipath.

Our approach for deriving the multipath observables is based on the use of two GPS receivers (a master and a slave) connected to the same clock to remove the common satellite and receiver clock biases after single differencing. It is possible to specify the relative dynamics between the antennas of the two receivers through a rotation motion, like that provided by a momentum wheel with a lever arm with a pre-chosen rotation speed, combined with the platform specific dynamics. This has two main advantages:

- A conventional approach uses a bundle of antennas, which share common multipath effects, in order to obtain redundancy for the multipath parameterization. In our approach, the relative receiver dynamics satisfies the initial system observability, based on the signature of the low-frequency multipath, geometry between the antennas, and the multipath profile. Thus, it reduces the number of antennas required, simplifying the system and making it more robust.
- Second, the relative receiver dynamics allows the calibration of the system not only for the derivation of the observables, adapting itself to the multipath environment, but also for related problems such as the ambiguity fixing, antenna phase-center variation and phase wind-up. Therefore, even before the platform starts navigating, the problem of initial low-frequency multipath and initial integer ambiguity resolution may be handled during the calibration mode.

Other initial concerns, besides the obvious validation of the observables for all possible sources of multipath spectra, are the system observability and the applicability in real-time scenarios. These are obvious problems, since the derivation of multipath observables is not straightforward, requiring some mathematical manipulations of the raw data before we can even derive the observable. Such manipulations should be performed continuously until the estimator converges towards the multipath profile (ending the calibration mode).

We performed initial tests to accurately validate the mathematical and stochastic signature of the multipath observables. This was performed through tests in different scenarios using a multipath software simulator for the GPS signal, and a calibrated motion table for real data. In this paper, we describe of the results of initial tests and address issues and problems of our approach, and discuss possible applicability in real-time scenarios.

We further address our future work including the multipath parameterization based on the profile and the full implementation of the estimator and thus the mitigation of multipath on carrier phase measurements. The approach will be extended to signals from pseudolites since, based-on preliminary simulations, we could see no major problem to extend it to indoor scenarios.

## INTRODUCTION

The limiting factor on performance in almost all precise differential carrier-phase applications is specular multipath, since it can account for at least 90 percent of

the total error budget [Comp and Axelrad, 1996]. Therefore, it is not a surprise that several research studies for hardware/software-based carrier-phase multipath mitigation techniques have already been developed, though in most of the cases, their use is limited to static applications.

However, carrier-phase kinematic applications involving low/medium dynamics, where the integer ambiguities must be sought in real-time, are of much more importance. Such applications may include precise navigation and surveying, machine guidance, attitude and control systems, geophysical studies, etc., and multipath appears to be a dominant error source in all these applications.

Most of the carrier-phase specular mitigation techniques developed for static applications takes advantage of the deterministic and correlated behaviour of the low-frequency multipath error. This correlation is induced by the reflector(s) in the vicinity and the satellite-antenna(s) relative geometry. The proximity of several antennas is used, for instance, to augment the observability and estimate the common static multipath effects at closely-spaced antennas [Ray et al., 1998]. These station-dependent multipath errors may also be decorrelated using a moving antenna(s) by means of a robot [Böder et al., 2001], knowing that the antenna(s) random motion shifts the systematic site-dependent multipath error to a high-frequency (decorrelated) multipath error.

Multiple site antennas and multipath decorrelation through antenna random motion, although applied to static or station-calibration techniques, have several limitations and shortcomings when we try to apply them to kinematic applications, where the antenna(s) is (are) positioned on a rover. In this paper, we describe how the synergy of these approaches is used to develop a new multipath observable (between antennas) that should clearly represent and absorb all the multipath spectra in kinematic scenarios.

Once the observable is sought, its geometric parameterization in order to be an effective or virtual reflector (between the antennas and the satellite), is recovered and the carrier-phase multipath error is mitigated for each antenna.

## MULTIPATH SPECTRA

Multipath refers to the existence of signals reflected from objects in the vicinity of a receiver's antenna that corrupt the line-of-sight signals from the GPS satellites. Particularly difficult is close-in multipath in which the reflected secondary signals arrive only slightly later (within about 100 nanoseconds or 30 metres), having

been reflected from objects only a short distance from the receiver antenna [Weill, 2003]. This short-delay, low-frequency multipath has a quasi-periodic behaviour, introducing a bias in the carrier-phase measurement, which is difficult to model or average out.

In a kinematic scenario, due to mobile antenna motion, the phase of the reflected signals randomly varies in the time domain with changes of mobile antenna location. This effect is equivalent to a random phase modulation, because the time derivative of phase appears as noise to the receiver [Blaunstein and Andersen, 2002]. An illustration of the multipath effects experienced by a static and a mobile antenna is given in Fig. 1.

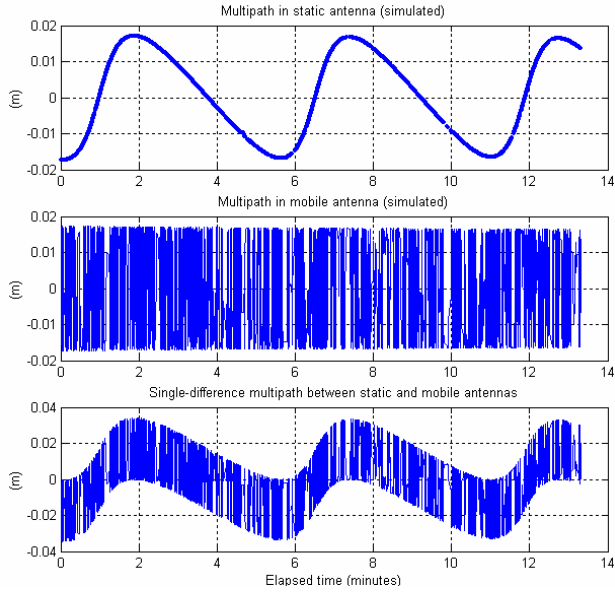


Figure 1: Carrier-phase multipath simulation for a static and mobile antenna and a particular satellite, using a nearby reflector.

The functional model for the carrier-phase multipath error (in the static antenna) is [Ray et al., 1999]:

$$M_m(t) \cong a \tan \left( \frac{\sum_{i=0}^n C_m(t) \mathbf{a}_R(t) \sin[\mathbf{f}_m(t) + \mathbf{g}_m^i(t)]}{\sum_{i=0}^n C_m(t) \mathbf{a}_R(t) \cos[\mathbf{f}_m(t) + \mathbf{g}_m^i(t)]} \right) \quad (1)$$

where  $C_m(t)$ ,  $\mathbf{a}_R(t)$ ,  $\mathbf{f}_m(t)$ , and  $\mathbf{g}_m(t)$  represent the correlation function (phase-lock loop), the reflection coefficient (reflector material dependent), the true carrier-phase observable (calculated, using for example, the unambiguous geometric range between the coordinates of the receiver antenna and a precise satellite ephemeris IGS-SP3 file), and the signal path delay, respectively.

For only one strong nearby reflector, which is the case in our simulations and real tests, the single difference multipath equation can be arranged in the following form [Ray et al., 1998]:

$$\Delta M_{m,s}(t) = M_m(t) - M_s(t) \cong a \tan \left( \frac{\mathbf{a}_i(t) \sin \mathbf{f}_m(t) - \mathbf{a}_i(t) \sin \mathbf{f}_s(t) + \mathbf{a}_i^2(t) \sin[\mathbf{f}_m(t) - \mathbf{f}_s(t)]}{1 + \mathbf{a}_i(t) \cos \mathbf{f}_m(t) - \mathbf{a}_i(t) \cos \mathbf{f}_s(t) + \mathbf{a}_i^2(t) \cos[\mathbf{f}_m(t) - \mathbf{f}_s(t)]} \right) \quad (2)$$

where  $m$  indicates the master antenna, and  $s$  the slave antenna. This is going to be the observable that we want to separate from the between-receiver carrier-phase raw measurements. If an observable can truly physically represent this quantity, then the multipath profile can be parameterized and an estimation of the reflector geometric parameters can be achieved. For our purposes, and before the parameterization of multipath, which will depend on the theoretical validation of the functional model (Eq. 2), this observable is going to be our workhorse.



Figure 2: Scenario for the multipath profile estimation, with a strong nearby reflector and two antennas (static and mobile).

Real tests were performed using this methodology. Using only two antennas (see Fig. 2), where the master antenna is fixed (thus only experiencing the satellite-platform dynamics) and the slave is mobile (thus superimposing its own dynamics on the one from the satellite-platform), one is merging the system observability augmentation with

the decorrelation of the multipath through a pseudo-random motion.

Decorrelation of multipath can be achieved using platforms with different pseudo-random motions. If the antennas experience a 3D rather than 2D pseudo-random motion, the decorrelation will be faster and more robust, since it will increase the subspace of all possible random multipath values in the time domain. Such a scenario can be realized, for instance, with a motion table (see Fig. 3).



Figure 3: Scenario for the multipath profile estimation, with a motion table.

A common-receiver external oscillator was used in the experiments to remove the receiver and satellite clock biases after differencing, resulting in the following equation:

$$\Delta\Phi_{m,s}^{prn}(t) = \Delta r_{m,s}^{sat}(t) + \Delta M_{m,s}^{sat}(t) + \Delta N_{m,s}^{sat}(t) + \Delta e_{m,s}^{sat}(t) \quad (3)$$

where  $\Delta r_{m,s}^{sat}(t)$  is the differential geometric range,  $\Delta M_{m,s}^{sat}(t)$  is the single-difference multipath error,  $\Delta N_{m,s}^{sat}(t)$  is the single-difference integer ambiguity and  $\Delta e_{m,s}^{sat}(t)$  is the system noise, all referred to the between antenna measurements (m: master; s: slave). Since the antennas are very close to each other, and the sampling rate is equal to or higher than 10 Hz, the first-order atmospheric errors do not appear in Equation 3.

Whilst the mobile antenna performs a pseudo-random motion, a bias with a magnitude of a quarter of a cycle may be introduced in the carrier-phase measurement (this magnitude will be clear later). However, the static (master) antenna also rotates with respect to an axis through its centre (spinning axis), thus experiencing the same phase wind-up effect. This common error will be

removed after performing a single-differencing. The exact extraction of a single-difference multipath measurement is successful only if the remaining biases contained in the carrier phase are also removed, thus the need for a common oscillator.

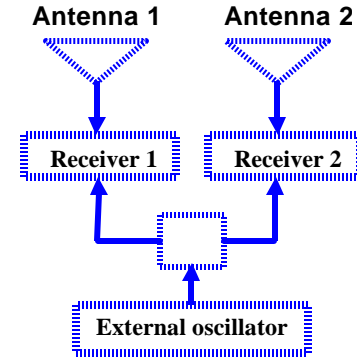


Figure 4: Hardware configuration for the studies performed, including an external oscillator.

In the next figure, one can see the results from the real-data test (using the test setup from Fig. 2).

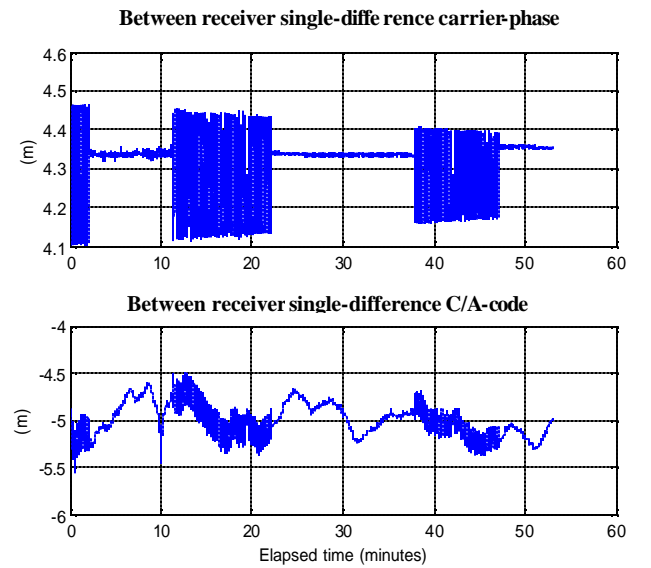


Figure 5: An example of measurements from the test scenario depicted in Fig. 2, for both carrier-phase and code-phase observables.

From Fig. 5, one can see that the external oscillator introduces a constant bias (coming from the hardware differential delay). However, this occurrence does not pose a problem since the multipath observable will be developed based on the between-antenna measurements differenced in time, thus eliminating this bias.

The thin noisy line represents Eq. 1 when both antennas are static. The oscillating one represents the same equation when the slave antenna performs a rotating

motion around the master antenna (2D pseudo-random motion).

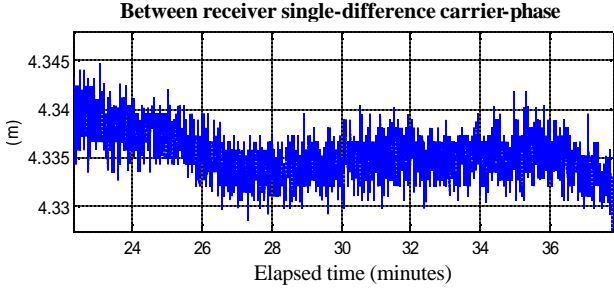


Figure 6: Zoom of the single-difference carrier-phase measurements when antennas are static.

To better understand the effect of the specular multipath error on carrier-phase measurements, we can zoom in on the periods when the antennas were static. Figures 6 and 7 depict such occurrences, and one can clearly see in them a low-frequency pattern with a period of a few minutes, plus some amplified noise from the differencing.

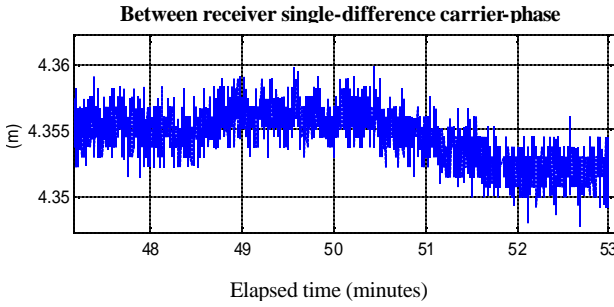


Figure 7: Zoom of the single-difference carrier-phase measurements when antennas are static.

In order to derive continuously the between-antenna multipath observable, only the periods when there's antenna-relative motion can be used. This is due to the multipath decorrelation and observability augmentation with the mobile antenna pseudo-random motion. The resultant single-difference carrier-phase measurement in these periods is depicted in the next figure:

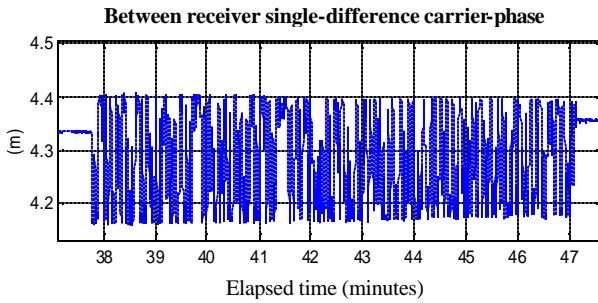


Figure 8: Zoom of the single-difference carrier-phase measurements when the mobile antenna is oscillating back and forth.

## MULTIPATH OBSERVABLES

Based on Eq. 1, we can further develop the equations in the following form, differencing them in time:

$$\begin{aligned} d\Delta\Phi_{m,s}^{sat}(t_k, t_{k-dt}) &\approx d\Delta r_{m,s}^{sat}(t_k, t_{k-dt}) \\ + d\Delta M_{m,s}^{sat}(t_k, t_{k-dt}) &+ d\Delta e_{m,s}^{sat}(t_k, t_{k-dt}) \end{aligned} \quad (5)$$

$$\begin{aligned} d\Delta M_{m,s}^{sat}(t_k, t_{k-dt}) &\approx d\Delta\Phi_{m,s}^{sat}(t_k, t_{k-dt}) \\ - d\Delta r_{m,s}^{sat}(t_k, t_{k-dt}) &- d\Delta e_{m,s}^{sat}(t_k, t_{k-dt}) \end{aligned} \quad (6)$$

where  $dt$  is the time latency between the epochs of integration. Obviously the biggest problem is in the determination of the quantity  $d\Delta r_{m,s}^{sat}(t)$ , which is unknown. However, this quantity can be integrated if one estimates the range-rate, range-acceleration and “range-jerk” (between antennas):

$$\begin{aligned} d\Delta M_{m,s}^{sat}(t_k, t_{k-dt}) &\approx d\Delta\Phi_{m,s}^{sat}(t_k, t_{k-dt}) \\ - \Delta\dot{r}_{m,s}^{prn}(t_{k-dt})dt &- \Delta\ddot{r}_{m,s}^{sat}(t_{k-dt})\frac{dt^2}{2} - d\Delta e_{m,s}^{sat}(t_k, t_{k-dt}) \end{aligned} \quad (7)$$

In this case, one must not only recover the unknown differenced-in-time single-difference geometric range, but also to have the guarantee that this quantity is really independent of the specular multipath.

If this is the case and it is achievable, then clearly the differenced-in-time single-difference multipath error will be isolated in the following equation:

$$\begin{aligned} d\Delta M_{m,s}^{sat}(t_k, t_{k-dt}) &\approx \sum_{i=k-dt}^k d\Delta\Phi_{m,s}^{sat}(t_i, t_{i-1}) \\ - \sum_{i=k-dt}^k \left[ \Delta\dot{r}_{m,s}^{sat}(t_{i-1})dt + \Delta\ddot{r}_{m,s}^{sat}(t_{i-1})\frac{dt^2}{2} \right] &- d\Delta e_{m,s}^{prn}(t_k, t_{k-dt}) \end{aligned} \quad (8)$$

From previous studies on GPS velocity and acceleration determination [Serrano et al., 2004], we showed that it is possible to achieve accuracies of a few mm/s and mm/s<sup>2</sup> depending on receiver quality, whether in static or kinematic mode, stand-alone or relative mode, and the particular dynamics situation, using the carrier-phase observable without solving for the integer ambiguities.



Figure 9 Setup of a NovAtel antenna on the top of a vehicle, for a kinematic test.

The velocity and acceleration of an antenna mounted on a moving platform can be determined by using the carrier-phase-derived Doppler (range-rate) and range-acceleration measurements.

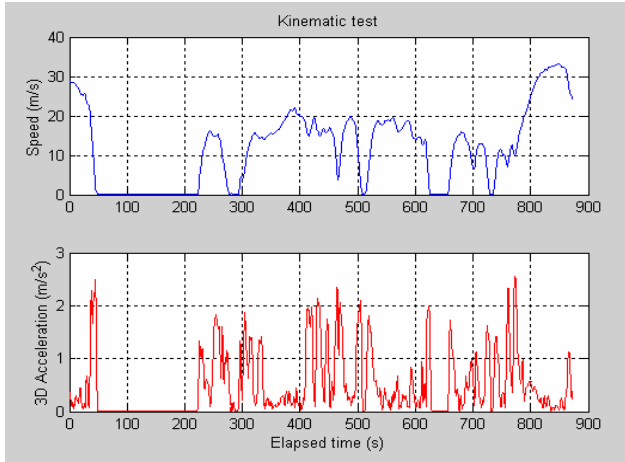


Figure 10: The GPS-derived speed and 3D acceleration under different dynamics during a kinematic test.

These measurements are modeled according to:

$$\dot{\Phi}_u^s = \mathbf{h}_u^s \cdot (\mathbf{v}_u - \mathbf{V}^s) + \dot{B}_u + \mathbf{e}_{u_\phi}^s \quad (9)$$

$$\ddot{\Phi}_u^s = \dot{\mathbf{h}}_u^s \cdot (\mathbf{v}_u - \mathbf{V}^s) + \mathbf{h}_u^s \cdot (\mathbf{a}_u - \mathbf{A}^s) + \ddot{B}_u + \mathbf{e}_{u_\phi}^s \quad (10)$$

where  $\mathbf{V}^s$  and  $\mathbf{A}^s$  stand for the satellite velocity and acceleration vectors;  $\mathbf{v}_u$  and  $\mathbf{a}_u$  for the receiver velocity and acceleration vectors; and  $\mathbf{h}$  represents the directional cosine vector between the receiver and satellite (see [Serrano et al., 2004] for derivation/discussion of these observables).  $\dot{B}_u$  and  $\ddot{B}_u$  represent the receiver clock-drift and drift-rate, which disappear after between-receiver differencing. Once the antenna velocity and

acceleration are estimated, one can derive the range-rate and range-accelerations:

$$\dot{r}_u^s = \mathbf{h}_u^s \dot{\mathbf{x}}_u^s \quad (11)$$

$$\ddot{r}_u^s = \dot{\mathbf{h}}_u^s \cdot \dot{\mathbf{x}}_u^s + \mathbf{h}_u^s \cdot \ddot{\mathbf{x}}_u^s \quad (12)$$

Based on Equation 8, and assuming that the measurements  $d\Delta M_{m,s}^{sat}(t)$  only reflect the decorrelation of the multipath through the between-antenna pseudo-random motion, these quantities are modeled as a random stochastic process. In this situation:

$$E\left\{\int d\Delta M_{m,s}^{sat}(t_k, t_{k-dt})\right\} \equiv E\left\{\int d\Delta M_{m,s}^{sat}(t_k, t_{k-1})\right\} - E\left\{\int \Delta M_{m,s}^{sat}(t_{k-dt})\right\} \quad (13)$$

where

$$E\left\{\int d\Delta M_{m,s}^{sat}(t_k, t_{k-1})\right\} = 0; E\left\{\int \Delta M_{m,s}^{sat}(t_{k-dt})\right\} = \Delta M_{m,s}^{sat}(t_{k-dt})$$

$$\text{therefore } E\left\{\int d\Delta M_{m,s}^{sat}(t_k, t_{k-dt})\right\} \equiv -\Delta M_{m,s}^{sat}(t_{k-dt})$$

which is exactly the observable we are looking for. This process can be done continuously recovering the single-difference multipath observables, and the amount of data necessary to randomize and estimate it epoch-by-epoch depends on many factors, including the kind of reflector, platform dynamics and motion, etc. Based on empirical studies using a multipath software simulator and this approach, one minute's worth of data (at 10 Hz data rate) was the minimum required.

## MULTIPATH SIMULATOR AND TESTS

To verify if one can actually separate the low-frequency multipath errors plus randomized multipath errors from the carrier-phase measurements using the approach described in the previous section, we developed a multipath software simulator using Matlab software.

In an attempt to mimic the real scenario from Fig. 2, we simulated a perfectly smooth reflector (see Fig. 11) in the vicinity of the antennas, and employing the multipath functional model from Equation 1, we obtained the simulated specular multipath effect at both antennas. The geometry relating the reflector to the antennas and satellite arc in this simulation are perfectly known ( $\hat{S}^i, \hat{S}^r, \mathbf{q}^i, \hat{n}$ , and  $\mathbf{a}_R$  are the unit direction vectors of the incident and reflected rays, the incident angle, the normal to the specular reflection point and the reflection coefficient respectively).

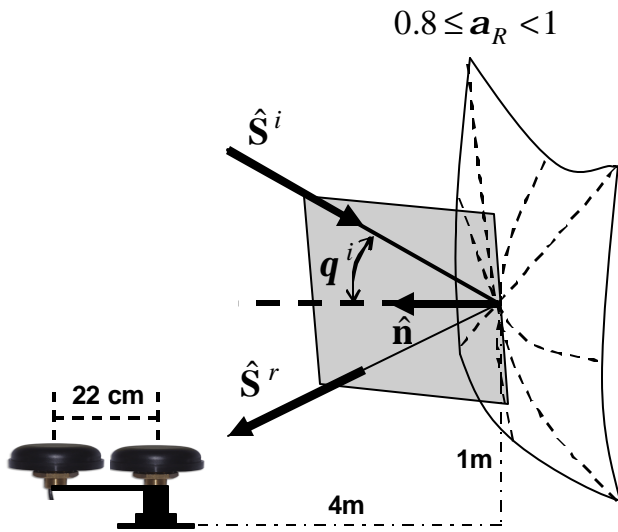


Figure 11: Simulated perfectly smooth reflector that reflects in all azimuth directions. Its geometry relative to the antennas/satellite and its material composition may be arbitrarily chosen (representative values are depicted in the figure).

The resultant simulated single-difference multipath between antennas is depicted in Figure 12. Only a two minute data span is plotted to make it easier to recognize the high-frequency multipath superimposed on the low frequency (specular) multipath.

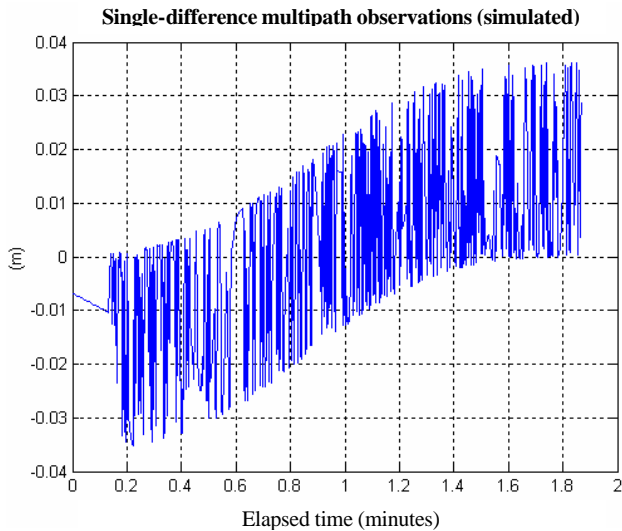


Figure 12: Single-difference multipath between antennas.

The position estimates of the master (static) antenna are depicted in the next figure. They were obtained by means of weighted least-squares estimation using the simulated carrier-phase measurements corrupted by the simulated static multipath. As expected, the effect of this error in the solution domain is reflected as a bias with a deterministic

quasi-periodic pattern, with considerable amplitude in the up component.

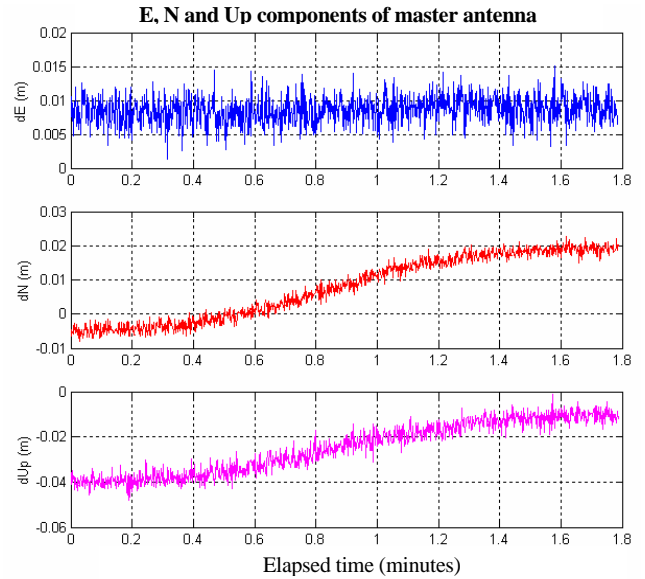


Figure 13: Local level coordinate system estimates of the static antenna position.

The mobile antenna, as explained before, has an imposed pseudo-random rotation motion around the static antenna. To simulate this motion, a random-walk for the between-antenna azimuth was used (using steps with standard deviation equal to  $90^\circ/s$ ), since the baseline length is fixed. Therefore, the random response from the multipath effect at the mobile antenna will be dependent of this choice of a stochastic process. The position results of the mobile antenna are depicted in the next figure:

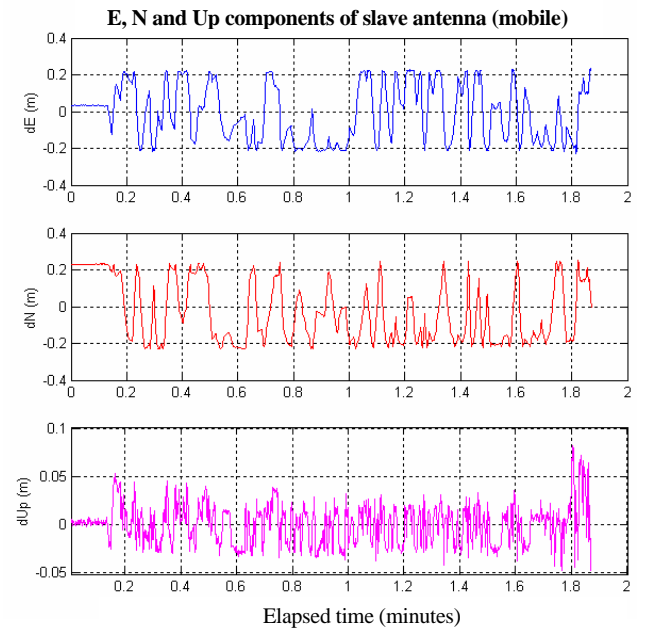


Figure 14: Local level coordinate system estimates of the mobile antenna position.

Obviously it is difficult to see the high-frequency multipath error contained in the solution domain results.

Nevertheless, the point is that in order to isolate the single-difference multipath, the between-antenna dynamics information (single-difference range-rate and range-acceleration) should be immune to the low-frequency part of the multipath. Most of this error will be hidden in the low-frequency components of the single-difference carrier-phase measurement and its variation in time.

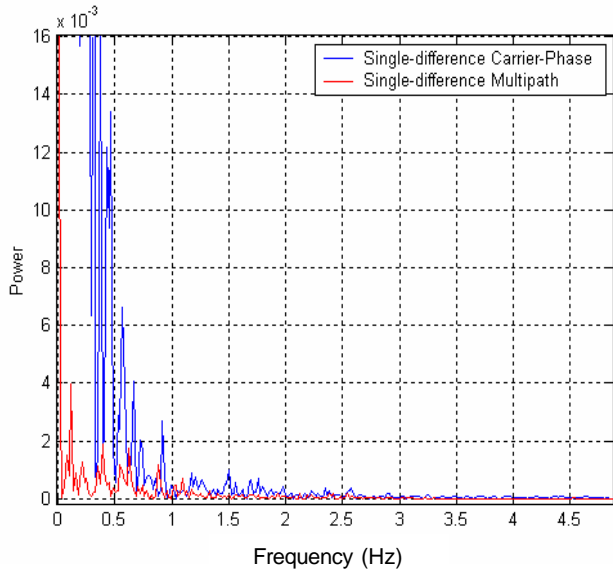


Figure 15: Frequency components of the simulated multipath and the corrupted carrier-phase measurements.

As one can see from Fig. 15, most of the low-frequency components of the simulated between-antenna multipath spectra overlap the low-frequency spectra of the simulated corrupted carrier-phase measurements. The carrier-phase rate will most likely contain some part of this spectrum.

Thus, the range-rates are essential in this process and the between-antenna velocity estimates should be regarded as the key to separate the low-frequency multipath. The high-frequency decorrelated multipath is not problematic and should be embedded in the range-acceleration and probably even the third-order range-jerk, depending on the dynamics.

Even though the range-rates could be derived directly from the differencing of the carrier-phase measurements (FIR filtering), i.e., in the measurement domain, nothing can guarantee that the specular multipath would be completely removed despite the use of high or band-pass filters

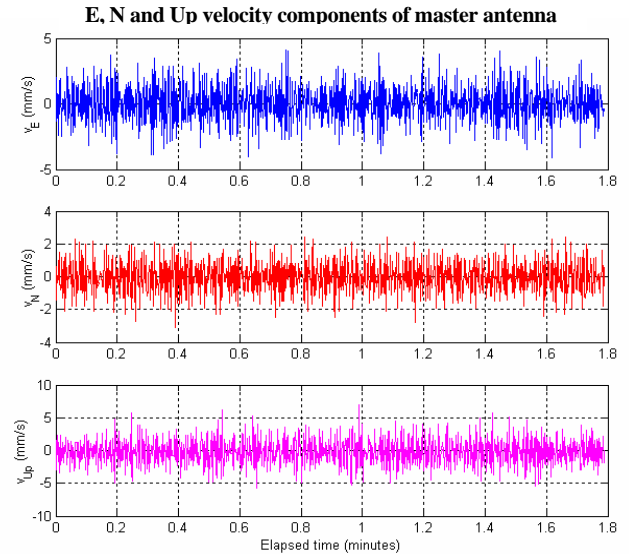


Figure 16: Local level system estimates of the master antenna velocity.

From the previous figure, one can see that the velocity estimates (i.e., in the solution domain) besides being precise at the mm/s level, are also free from multipath bias.

Estimating the velocity in the solution domain and then recovering the line-of-sight range-rate, makes use of at least 4 satellite measurements with different range-rates corrupted by different multipath spectra. Besides, the least-squares velocity estimation is in itself already a whitening process, especially when decorrelating the site-antenna-satellite multipath signature.

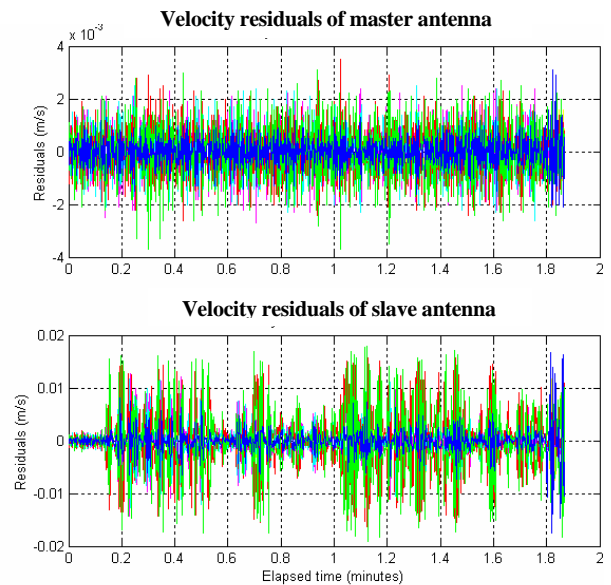


Figure 17: Velocity estimation residuals (top: static antenna; bottom: mobile antenna).

That can also be seen in the static antenna residual plots (Fig. 17 - top panel), whereas in the mobile antenna velocity residuals, one can see clearly the effect of the high-frequency multipath acting as amplified noise (Fig. 17 - bottom panel). This comes from the differencing of the carrier-phase measurements corrupted by randomized multipath, which amplifies the noise level. The results in the solution domain, i.e., the mobile-antenna velocity estimates (Fig. 18), not only show some of this amplified random noise especially in the up component (which should be zero), but also an error in the estimation of the sudden dynamics change (aliasing). Clearly the velocity and acceleration estimator for the mobile antenna does not meet the requirement of a pseudo-random motion with unknown dynamics involved (jerk included).

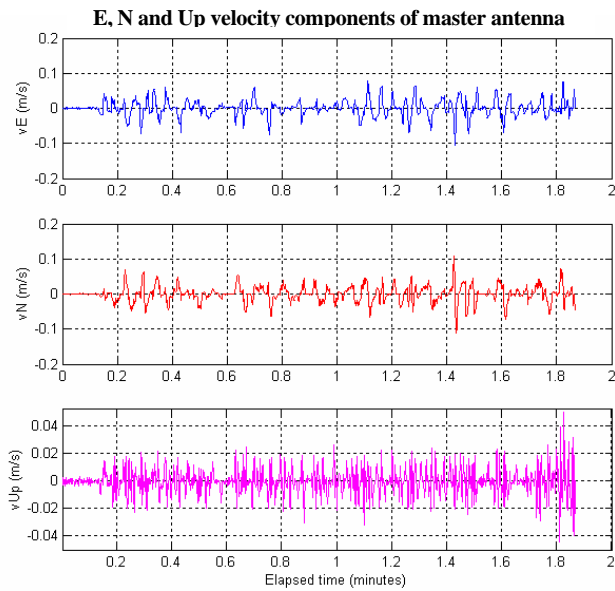


Figure 18: Local level system estimates of the mobile-antenna velocity.

This is obvious when deriving the multipath observable from an ensemble of several measurements (Eq. 8), which depends on the precise and accurate estimation of the between-antenna dynamics. The first requirement, i.e., separation of the low-frequency multipath component from the static antenna response is fulfilled. The second one, the exact determination of the mobile-antenna dynamics is not, thus some of these errors are passed as non-linearities to the differenced-in-time, single-difference multipath measurements (Fig. 19).

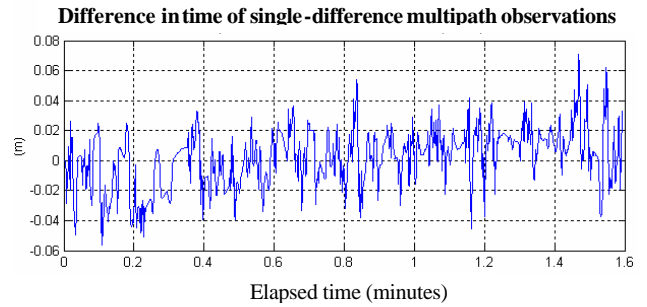


Figure 19: Just an example from a satellite in investigation, of differenced-in-time single-difference multipath observations, necessary to estimate the between-antennas multipath at a specific epoch.

These non-linearities are clear in the figure, which should ideally reflect a linear random-process centered on the numerical value of the multipath observable to be estimated. When calculating the ensemble expected value using Eq. 13 (using for instance, estimators of the mean of a random variable) some errors are introduced, though random in nature and not corrupted by the specular multipath. In the next figure, one can see the results from our approach for continuously deriving single-difference multipath observations.

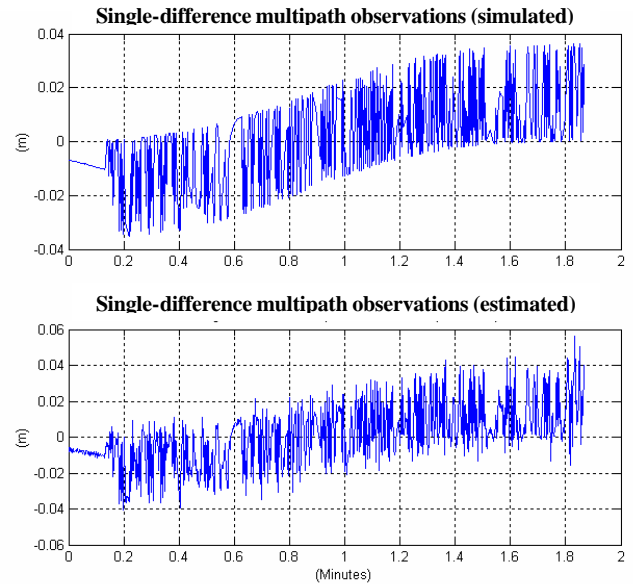


Figure 20: Between-antenna multipath observations (top: simulated; bottom: estimated).

The estimated between-antenna multipath observables clearly have a structure similar to the simulated values. Most of the errors (Fig. 21) represent the randomized high-frequency multipath errors and the imperfect dynamics estimation for the mobile antenna (higher-order dynamics such as “range-jerks” were not estimated). Most important, they do not show evidence of any significant

biases, though the noise has a high-correlation with the mobile-antenna dynamics.

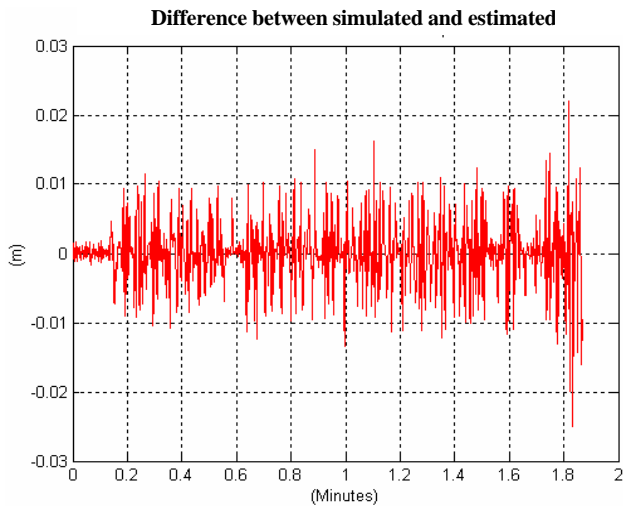


Figure 21: Errors between simulated and estimated single-difference multipath measurements.

This approach could be extended to a platform with slow motion, where one antenna was static in relation to the platform and the other mobile antenna performing a calibration routine. Once this step was fulfilled, then the navigation stage could start though accompanied with a change in the multipath environment. But, as long as the calibration stage is successful and multipath observables continue to be estimated, then multipath parameterization in the navigation mode can also be achieved.

## CONCLUDING REMARKS

We presented a new approach for deriving a multipath observable that should, in principle, represent the true multipath spectra and not simply a representative observation (e.g. SNR measurements). This approach is devised for GPS-RTK applications and only uses two antennas, which simplifies the system and its applicability to the rover platform.

The multipath software simulations were designed to provide “observables” as close as possible to the true possible multipath values in a real observed scenario.

The derivation of the single-difference multipath observables is carried out in the solution domain because of the ease of multipath decorrelation. The disadvantage of this approach is that it needs at least 4 simultaneous satellite measurements, whereas in the measurement domain, only the signal from the one satellite under investigation is necessary to build the multipath profile. In urban environments, this is a drawback.

Based on the preliminary tests using data generated by a software simulator, the approach was effective though

with some limitations. Higher-order mobile-antenna dynamics should be studied and modelling improved, in order to reduce the randomization time (~ 1 minute) but being capable at the same time of recovering the mobile antenna dynamics.

The functional model for the simulated single-difference multipath error performed quite well. Nevertheless, it should be studied with more realistic scenarios, i.e., a variable number of effective reflectors, materials with different reflection characteristics, different receiver-dependent PLL correlation functions and multipath geometrical signal delay.

## FURTHER RESEARCH

The multipath simulator will be improved with some of the changes described in the previous section. Diffraction should also be included and studied to verify its spectra and signature among the recovered multipath observables.

We will also develop functional models for the real-time determination of “range-jerks” (both in the measurement and solution domains). Such modelling is crucial when the relative between-antenna motion is embedded in the platform motion (thus subject to multiple acceleration variations).

Different platform scenarios should be studied, complemented by the respective model. Especially important are those scenarios where the platform has dynamics and the effective reflector’s positions change in a shorter time span than in a static scenario, thus changing constantly the multipath profile and parameterization.

## ACKNOWLEDGMENTS

The work described in this paper was supported in part by the Natural Sciences and Engineering Research Council of Canada and the Canadian Space Agency.

## REFERENCES

- Blaunstein, N. and J. B. Andersen (2002). *Multipath Phenomena in Cellular Networks*. Artech House, Inc., Norwood, MA; 296 pp.
- Böder, V., F. Menge, G. Seeber, G. Wübbena and M. Schmitz (2002). “How to Deal with Station Dependent Errors – New Developments of the Absolute Field Calibration of PCV and Phase-Multipath With a Precise Robot”. Proceedings of ION GPS 2001, Salt Lake City, Utah, 11-14 September 2001; pp. 2166-2176.

- Bruton, A. M., C. L. Glennie and K. P. Schwarz (1999). “*Differentiation for High-Precision GPS Velocity and Acceleration Determination*”. GPS Solutions, Vol. 2, No. 4; pp. 4-21.
- Byun, S. H., G. A. Hajj and L. E. Young (2002). “*GPS Signal Multipath: A Software Simulator*”. GPS World, Vol. 13, No. 7, July; pp. 40-49.
- ICD-GPS-200C (1999). *Navstar GPS Space Segment/Navigation User Interface Control Document*, GPS Navstar JPO; 138 pp.
- Jekeli, C. and R. Garcia (1997). “*GPS Phase Accelerations for Moving-base Vector Gravimetry*”. Journal of Geodesy, Vol. 71, No. 10; pp. 630-639.
- Jin, X. (1996). *Theory of Carrier Adjusted DGPS Positioning Approach and Some Experimental Results*. Delft University Press, Delft, The Netherlands; 162 pp.
- Kaplan, E. D. (Ed.) (1996). *Understanding GPS, Principles and Applications*, Artech House Publishers, Boston-London; 554 pp.
- Kennedy, S. (2002). “*Precise Acceleration Determination from Carrier Phase Measurements*”. Proceedings of ION GPS 2002, Portland, Oregon, 24-27 September 2002; pp. 962-972.
- Kim, D. and R.B. Langley (2003). “*On Ultrahigh-Precision Positioning and Navigation*”. Navigation: Journal of the Institute of Navigation, Vol. 50, No. 2, Summer; pp. 103-116.
- Misra, P. and P. Enge (2001). *Global Positioning System: Signals, Measurements, and Performance*. Ganga-Jamuna Press, Lincoln, Massachusetts ; 390 pp.
- Ray, J. K., M. E. Cannon and P. Fenton (1998). “*Mitigation of Static Carrier Phase Multipath Effects Using Multiple Closely-Spaced Antennas*”. Proceedings of ION GPS 1998, Nashville, Tennessee, 15-18 September 1998; pp. 1025-1034.
- Ray, J. K. and M. E. Cannon (1999). “*Characterization of GPS Carrier Phase Multipath*”. Proceedings of ION NTM 1999, San Diego, California, 25-27 January 1999; pp. 343-352.
- Serrano, L., D. Kim and R.B. Langley (2004). “*A GPS Velocity Sensor: How Accurate Can It Be? – A First Look*”. Proceedings of ION NTM 2004, San Diego, California, 26-28 January 2004; pp. 875-885.
- Serrano, L., D. Kim and R.B. Langley (2004). “*A Single GPS Receiver as a Real-Time, Accurate Velocity and Acceleration Sensor*”. Proceedings of ION GNSS 2004, Long Beach, California, 21-24 September 2004; pp. 2021-2034.
- Van Graas, F. and A. Soloviev (2003). “*Precise Velocity Estimation Using a Stand-Alone GPS Receiver*”. Proceedings of ION NTM 2003, Anaheim, California, 22-24 January 2003; pp. 262-271.
- Weill, L. R. (2003). “*Multipath Mitigation: How Good Can It Get with New Signals*” GPS World, Vol. 16, No. 6, June; pp. 106-113.
- Zhang J., K. Zhang, R. Grenfell and R. Deakin (2003). “*Real-time GPS Orbital Velocity and Acceleration Determination in ECEF System*”. Proceedings of ION GPS/GNSS 2003, Portland, Oregon, 9-12 September 2003; pp. 1288-1296.